Nov 24th, 12:00 AM

Postbuckling Behaviour of a Webplate under Partial Edge Loading

Debal K. Bagchi

K. C. Rockey

Postbuckling Behaviour of a Webplate under Partial Edge Loading

by

Debal K. Bagchi[1]

&

Kenneth C. Rockey[2]

INTRODUCTION

The buckling of rectangular plates under the action of uniformly distributed compressive stresses, shear stresses and combinations of these loading systems have been extensively studied and the results are well documented (1-2).

A number of researchers (3-8), including the present authors, have provided solutions for the buckling of a panel of a plate girder when it is subjected to a partial edge load, such as that which occurs when the edge of the panel is subjected to the action of a wheel load. These solutions have resulted in the availability of design charts which enable engineers to readily determine the buckling load of panels subjected to partial edge loading.

However, a thin webplate subjected to a partial edge load has the ability to support loads far in excess of that which cause the plate to buckle.

[1]STRUCTURAL ENGINEER, Stone & Webster Engineering Corporation, Cherry Hill, New Jersey.

[2]PROFESSOR, Department of Civil & Structural Engineering, University College, Cardiff, U.K.

Rockey et al (9), Walker and Khan (8), Skaloud et al (10,11) and others (7,12,13) have examined experimentally this post buckled action and various rules are now available which enables one, for certain types of construction, to predict the collapse load of webs loaded by an edge patch load. In contrast, comparatively little theoretical work has been carried out to determine the post buckled action of webs when subjected to the loaded action of a patch edge load. This is due to the complex stress distribution that occurs in the webplate close to the loads. The present paper presents the results of a large deflection finite element solution which has been carried out by the authors.

The theoretical results obtained from the finite element solution are then compared with experimental results obtained from the authors experimental studies and that of other investigators.

THEORETICAL DEVELOPMENT

Formulation of Incremental Force-Displacement Relationship for an Element

A typical uniform finite element idealization of a rectangular plate is given in Fig. 1(a), with one typical element identified as ijkl. Fig. 1(b) gives the co-ordinate system which is employed when dealing with an element such as ijkl. The geometry of each element, whether triangular or rectangular is determined by straight lines joining the nodal points. The local orthogonal cartesian co-ordinates associated with individual elements are denoted as x, y, z. Similarly the displacements in terms of local co-ordinates are specified as u, v, w. The global axis system for the whole structure is denoted by the capital symbols as X, Y, Z. Considering the deflected form of an element when the external load is applied, the components of non-linear strain (14) in terms of local co-ordinates for a thin plate in bending can be written as :

$$
\begin{aligned}
e_{xx} &= \frac{\partial u}{\partial x} - z\,\frac{\partial^2 w}{\partial x^2} + \frac{1}{2}\left(\frac{\partial w}{\partial x}\right)^2 \;; \\
e_{yy} &= \frac{\partial v}{\partial y} - z\,\frac{\partial^2 w}{\partial y^2} + \frac{1}{2}\left(\frac{\partial w}{\partial y}\right)^2 \;; \\
e_{xy} &= \frac{\partial u}{\partial y} + \frac{\partial v}{\partial x} - 2z\,\frac{\partial^2 w}{\partial x.\partial y} + \frac{\partial w}{\partial x}\cdot\frac{\partial w}{\partial y} \;.
\end{aligned}
\tag{1}
$$

The above strain components can be separated into linear and non-linear strains and written in matrix form as shown below :

$$
\{e\} = \begin{Bmatrix} e_{xx} \\ e_{yy} \\ e_{xy} \end{Bmatrix} = \begin{Bmatrix} \dfrac{\partial u}{\partial x} - z\,\dfrac{\partial^2 w}{\partial x^2} \\ \dfrac{\partial v}{\partial y} - z\,\dfrac{\partial^2 w}{\partial y^2} \\ \dfrac{\partial u}{\partial y} + \dfrac{\partial v}{\partial x} - 2z\,\dfrac{\partial^2 w}{\partial x.\partial y} \end{Bmatrix} + \frac{1}{2}\begin{bmatrix} \dfrac{\partial w}{\partial x} & 0 & 0 \\ 0 & \dfrac{\partial w}{\partial y} & 0 \\ 0 & 0 & \sqrt{2}.\dfrac{\partial w}{\partial x} \end{bmatrix}\begin{Bmatrix} \dfrac{\partial w}{\partial x} \\ \dfrac{\partial w}{\partial y} \\ \sqrt{2}\,\dfrac{\partial w}{\partial y} \end{Bmatrix}
\tag{2}
$$

The stress/strain relation for a material obeying Hooke's law can be written as :

$$
\{\sigma\} = [C]\;\{e\} \;;
\tag{3}
$$

where $\{\sigma\} = \begin{Bmatrix} \sigma_{xx} \\ \sigma_{yy} \\ \sigma_{xy} \end{Bmatrix}$, and $[C]$ is a (3x3) square matrix containing the elastic constants.

Fig. 2 states the sign convention employed with a rectangular element. There are 6 displacements at each of the nodes, 3 translations and 3 rotations, see equation (4), which defines the 6 displacements at a node i.

$$\{q_i\} = \begin{Bmatrix} u_i \\ v_i \\ w_i \\ \Theta_{xi} \\ \Theta_{yi} \\ \Theta_{zi} \end{Bmatrix} = \begin{Bmatrix} q_{pi} \\ \cdots\cdot \\ q_{bi} \\ \cdots\cdot \\ \Theta_{zi} \end{Bmatrix} \tag{4}$$

where

$$\{q_{pi}\} = \begin{Bmatrix} u_i \\ v_i \end{Bmatrix} \quad ; \quad \{q_{bi}\} = \begin{Bmatrix} w_i \\ \Theta_{xi} \\ \Theta_{yi} \end{Bmatrix}$$

The column matrix $\{q\}$ represents the total number of displacement components of an element and can be written as :

$$\{q\} = \begin{Bmatrix} q_p \\ q_b \\ \Theta_z \end{Bmatrix} \tag{5}$$

where

$\{q_p\}$ = a column matrix representing the in-plane linear displacements of an element ;

$\{q_b\}$ = a column matrix representing the lateral component w and the rotational components Θ_x and Θ_y of an element ;

$\{\Theta_z\}$ = a column matrix representing in-plane rotational components, Θ_z of an element.

Similarly the force components acting at a node i are given by :

$$\{F_i\} = \begin{Bmatrix} F_{xi} \\ F_{yi} \\ F_{zi} \\ M_{xi} \\ M_{yi} \\ M_{zi} \end{Bmatrix} = \begin{Bmatrix} F_{pi} \\ F_{bi} \\ M_{zi} \end{Bmatrix} \tag{6}$$

The column matrix {F} representing the total components of forces acting at all nodes of an element is given by :

$$\{F\} = \begin{Bmatrix} F_p \\ F_b \\ M_z \end{Bmatrix} \tag{7}$$

where,

$\{F_p\}$ = in-plane direct force components of an element;
$\{F_b\}$ = lateral force, F_{zi} and moment components M_{xi} and M_{yi} of an element;
$\{M_z\}$ = moment components M_{zi} of an element.

The displacement functions for u, v and w can be written in the following form :

$$\begin{aligned} u &= \phi^u(x,y).\alpha \\ v &= \phi^v(x,y).\alpha \\ w &= \phi^w(x,y).\beta \end{aligned} \tag{8}$$

where,

$\{\alpha\}$ = a column matrix representing arbitrary constants; the total number of constants being equal to the total number of in-plane freedom of an element denoted by $\{q_p\}$;

$\{\beta\}$ = a column matrix representing arbitrary constants, the total number of constants being equal to the total number of lateral and rotational components denoted by $\{q_b\}$.

Substituting the values of nodal co-ordinates in the equation (8), one can rewrite the displacement functions in the form :

$$\begin{Bmatrix} u \\ v \\ w \end{Bmatrix} = \begin{bmatrix} \phi^u \cdot B_p^{-1} & 0 & 0 \\ \phi^v \cdot B_p^{-1} & 0 & 0 \\ 0 & \phi^w \cdot B_p^{-1} & 0 \end{bmatrix} \begin{Bmatrix} q_p \\ q_b \\ \theta_z \end{Bmatrix} \quad ; \qquad (9)$$

where, $\phi^u = \phi^u(x,y)$; $\phi^v = \phi^v(x,y)$ and $\phi^w = \phi^w(x,y)$; and B_p, B_b are square matrices relating arbitrary constants with the displacement components. Substituting the values of displacements u, v, and w from the equation (9) into equation (2), the strain vector $\{e\}$ can be written as :

$$\{e\} = \left[f_1\right]\{q\} + \begin{bmatrix} q_b & 0 & 0 \\ 0 & q_b & 0 \\ 0 & 0 & q_b \end{bmatrix}^T \left[f_{nx}^D\right]^T \left[f_{ny}\right] \{q_b\} \qquad (10)$$

where,

$$f_1 = \begin{bmatrix} \phi^u,x.\ B_p^{-1} & -z.\ \phi^w,xx.B_b^{-1} & 0 \\ \phi^u,y.\ B_p^{-1} & -z.\ \phi^w,yy.B_b^{-1} & 0 \\ \frac{1}{2}(\phi^u,y + \phi^u,x)\ B_p^{-1} & -z.\ \phi^w,xy.B_b^{-1} & 0 \end{bmatrix} ;$$

$$f_{nx}^D = \begin{bmatrix} \phi^w,x.B_b^{-1} & 0 & 0 \\ 0 & \phi^w,y.B_b^{-1} & 0 \\ 0 & 0 & \sqrt{2}.\ \phi^w,x.B_b^{-1} \end{bmatrix} ; \text{ and } \left[f_{ny}\right] = \begin{bmatrix} \phi^w,x.B_b^{-1} \\ \phi^w,y.B_b^{-1} \\ \sqrt{2}.\phi^w,y.B_b^{-1} \end{bmatrix}$$

Considering the two neighbouring positions of equilibrium of the elastic body shown in Fig. (3) designated as $(\ )^1$ and $(\ )^2$ and applying the principles of virtual work, one obtains

$$\delta(R_1)^1 + \delta(R_2)^2 = \delta(U)^1 \tag{11}$$

$$\delta(R_1)^1 + \delta(R_2)^2 = \delta(U)^2 \tag{12}$$

where,

R_1 = work done by the external forces in displacing the body from its initial position of equilibrium to its final position;

R_2 = work done by the body forces when it goes through the above displacements.

In the discrete-element solution the body forces, and also the external forces, are represented by their components acting at the nodal points. Therefore, the total work done by both the external and body forces are given by :

$$(R_1)^1 + (R_2)^1 = \int_0^q \{F\}^T . d\{q\} \tag{13}$$

where,

$\{F\}$ = a column vector representing nodal forces of an element;

$\{q\}$ = a column vector representing the nodal displacements of an element.

The strain-energy U developed in the elastic body during the above displacements, can be written as :

$$U = \frac{1}{2}\int_V \{e\}^T . \{\sigma\} dv \tag{14}$$

The expression for the incremental force displacement relationship when the body moves from the first position of equilibrium to the second position is obtained from the equations (2), (10), (11), (12), (13) and (14), and is given by :

$$\{\Delta F\} = \int_v \left[f_1\right]^T \left[\ C\ \right] \left[f_1\right] .dv.\ \{\Delta q\} \quad + \\ \int_v \left[f^D_{nx}\right]^T \left[\sigma^D\right] \left[f_{ny}\right] .dv.\ \{\Delta q\} \tag{15}$$

where

$$\left[\sigma^D\right] = \begin{bmatrix} \sigma_{xx} & 0 & 0 \\ 0 & \sigma_{yy} & 0 \\ 0 & 0 & \sigma_{xy} \end{bmatrix} .$$

Details of calculations leading to the equation (15) are given in the reference (15).

The first term of equation (15) represents the usual elastic linear stiffness matrix. The second term is defined as the geometric stiffness matrix for an element. Denoting the two above terms by the symbols $\left[K^e_E\right]$ and $\left[K^e_G\right]$, equation (15) is written as :

$$\{\Delta F\} = \left[K^e_E\right] \{\Delta q\} + \left[K^e_G\right] \{\Delta q\} = \left[K^e\right] \{\Delta q\} \tag{16}$$

The derivation of elastic and geometric stiffness matrices for rectangular elements is given below :

<u>Elastic Stiffness Matrix</u> $\left[K^e_E\right]$

Substituting the value of $\left[f_1\right]$ from equation (10) into equation (15), the elastic stiffness matrix can be written as :

$$\left[K_E^e\right] = \left[B_p^{-1}\right]^T \int_v \left[\phi^u{,}_x \phi^v{,}_y \ \tfrac{1}{2}\ (\phi^u{,}_y+\phi^v{,}_x)\right]^T \left[C\right] \begin{bmatrix} \phi^u{,}_x \\ \phi^v{,}_y \\ \frac{1}{2}(\phi^u{,}_y+\phi^v{,}_x) \end{bmatrix} .dv. \left[B_p^{-1}\right]$$

$$+ \left[B_b^{-1}\right] \int_v z^2 \left[\phi^w{,}_{xx} \phi^w{,}_{yy} \phi^w{,}_{xy}\right]^T \left[C\right] \begin{bmatrix} \phi^w{,}_{xx} \\ \phi^w{,}_{yy} \\ \phi^w{,}_{xy} \end{bmatrix} .dv. \left[B_b^{-1}\right] \qquad (17)$$

The first term in the equation (17) represents the in-plane stiffness denoted by K_E^{ep} ; the second term represents the bending stiffness of an element and denoted by K_E^{eb} .

In the present investigation, the following displacement functions due to Zienkiewicz and Cheung (16) have been used :

$$\begin{aligned} u(x,y) &= \alpha_1 + \alpha_2 x + \alpha_3 y + \alpha_4\ x\ y \\ v(x,y) &= \alpha_5 + \alpha_6 x + \alpha_7 y + \alpha_8\ x\ y \qquad (18) \\ w(w,y) &= \beta_1 + \beta_2 x + \beta_3 y + \beta_4 x^2 + \beta_5\ xy + \beta_6 y^2 \\ &\quad + \beta_7 x^3 + \beta_8 x^2 y + \beta_9\ xy^2 + \beta_{10}\ y^3 + \beta_{11}\ x^3 y + \beta_{12}\ xy^3 . \end{aligned}$$

Geometric Stiffness Matrix $\left[K_G^e\right]$

Substituting the values from (10) into equation (15), the geometric stiffness matrix $\left[K_G^e\right]$ can be written as :

$$\left[K_G^e\right] = \left[B_b^{-1}\right]^T \left[K_{xx} + K_{yy} + K_{xy}\right] \left[B_b^{-1}\right] \qquad (19)$$

where

$$\begin{aligned} K_{xx} &= \int_v \sigma_{xx} . \phi^w{,}_x{}^T .\phi^w{,}_x . dv ; \\ K_{yy} &= \int_v \sigma_{yy} . \phi^w{,}_y{}^T .\phi^w{,}_y . dv ; \\ K_{xy} &= \int_v \sigma_{xy} . \phi^w{,}_x{}^T .\phi^w{,}_y . dv . \end{aligned}$$

The three components of the geometric stiffness matrix denoted by K_{xx}, K_{yy} and K_{xy} are calculated from the displacement function given by the equation (18) for uniform stress-condition (15).

Formulation of the Overall-Matrix

The incremental force-displacement relationship for an element given by equation (16) when transformed from the local axis to the global co-ordinates becomes :

$$\{\Delta P_e\} = [R]^T [K^e] [R] \{\Delta Q_e\} \; ; \tag{20}$$

where

$\{\Delta P_e\}$ = a column matrix representing the components of the forces acting at nodal points of an element in global co-ordinates;

$\{\Delta Q_e\}$ = a column matrix representing the displacement components of an element in global co-ordinates;

$[R]$ = a transformation matrix relating local axis system with global co-ordinates.

The overall matrix is formed from the assembly of the individual stiffness matrices of elements and is given by :

$$\{\Delta P\} = [K]\{\Delta Q\} \tag{21}$$

RESULTS

Post-Buckling Behaviour of a Square Plate Loaded in Edge Compression

In this section, solutions are presented for the post buckling behaviour of a clamped square plate subject to uniform in-plane compressive stress acting on two opposite edges.

All four edges of the plate are fully restrained against out of plane rotation. The loaded edges remain straight and do not rotate in the plane of the plate when the plate is loaded, i.e. the loaded edges remain parallel to each other. The unloaded edges are allowed to move freely in the plane of the plate. The plate is assumed to have an initial deformation of the same form as that developed in the buckled plate; the central deflection having a magnitude of 0.2 times the thickness of the plate. The result of the finite element analysis is shown as curve 1 in Fig. 4.

Curves IIa and IIb are the two solutions obtained by Yamaki (17). In both solutions the loaded edges were constrained to remain straight and move with a parallel motion. The solution given by the curve (IIa) was obtained for the case where the unloaded edges are constrained to remain straight, whereas for case (IIb) the unloaded edges were allowed to move in the plane of the plate. The finite element solution gives better agreement with the case (IIa) compared to (IIb) although the differences between the two curves (IIa) and IIb) are not very significant. It should be mentioned that the present incremental approach calculated the membrane stress at the centroid of an element and not at the edge of the plate; and therefore with the present elements one cannot obtain the true stress-free condition. Also, since the stress component σ_y perpendicular to the unloaded edge is tensile, it is to be expected that the present solution will give a lower value for deflection as compared with the case where the edges are totally unconstrained (case (IIb)).

Fig. 5 gives a plot of the membrane stresses at the point marked A in the Fig. 4 in the x and y directions respectively. Also plotted in the same figure are the available experimental and theoretical values of Yamaki at the centre of the plate. Because of the initially deformed shape, the finite element solution shows closer agreement with experimental results than the theoretical values obtained by Yamaki for the case of a flat plate.

Post Buckling Behaviour of a Clamped Plate Under Partial Edge Loading

(a) Finite Element Solution:

Figs. 6-9 show the results obtained on the postbuckling behaviour of a clamped plate by the finite element method using rectangular elements. The dimensions of the plate are shown in the Fig. 6. The boundary conditions used for finite element analysis can be stated as follows :

(i) all the edges are free to move in the plane of the plate;

(ii) all the edges are clamped against lateral rotation;

(iii) the plate is supported vertically on two rollers placed at each end. The load P is applied centrally acting over a width of 3 inches on the top face of the plate. The load deflection behaviour of this plate along the central vertical line is shown in Fig. 6. The deflected form at P = O represents the initial curvature of the plate with a maximum deflection, W_o, at the centre equal to 0.3 times the thickness of the plate. The growth of deflection clearly shows that the crest at which the deflection is maximum moves away from the neutral axis with each increase in loading. Fig. 7 shows the load deflection behaviour at the point marked A in the Fig. 6. Figs. 8 and 9 show the growth of the membrane stresses σ_x and σ_y along the same vertical line with increase in loading. The actual values of the loads at which stresses are plotted are given in the Fig. 6.

(b) Experimental Results

A number of tests were conducted on panels of three different aspect ratio to study the postbuckling behaviour of the web under partial edge loading. Strain gauges are fixed at different locations at the central vertical line to measure membrane strains with the increase in loading. Details of the experimental set up are described elsewhere (8,15), and will not be described in detail in this paper. Fig. 10 gives the relevant details regarding the size of the girders and the type of loading employed, see also Fig. 11.

Figs. 12 - 17 show the experimental results obtained from the tests on three specimens. These results can be divided into two groups:

(i) Figures 12-14 show the membrane strain distribution along the central line for a given loading for the three test specimens. The locations at which the strains were measured are also shown in the corresponding figures. The membrane strains were calculated from the average value of two strain readings on opposite faces at a given location. Also, plotted in the same figures shown by the full lines are the values obtained by the finite element method along a vertical line very close to the central line. Generally, there is excellent agreement between the finite element result and the experimental results.

Figs. 15-17 show the load deflection behaviour of the three specimens at the location marked A in the corresponding figures. The buckling loads for an ideal plate obtained from the authors Finite Element Method are also shown in the corresponding figures. Clearly, in all cases failure has occurred after plastic deformation has occurred. In Fig. 15, the load/deflection relationship for the point marked A is compared with the finite element solution results given in the Fig. 6, and once again an excellent agreement has been obtained. Local yielding started at a load close to the critical load under the point of application of the loading on one face of the specimen. After this yielding has started, the plate deflection has grown very rapidly with increase of loading. This early yielding was due to the presence of the residual stress which are present and also due to initial curvature of the plate. A future extension of the present work will be to extend the present elastic postbuckling analysis to include plasticity.

CONCLUSION

The present paper presents a large deflection elastic finite element solution for the behaviour of a plate loaded by a patch load. Comparison is then made with existing experimental results and additional tests by the authors. A high level of agreement was obtained with the theoretical and experimental results.

ACKNOWLEDGEMENTS

The authors wish to thank the Steel Company of Wales for the financial assistance which enabled them to carry out this research work.

APPENDIX II-NOTATION

Notation

x, y, z	rectangular co-ordinates
t	thickness of plate element
u, v, w	components of displacements in x,y and z co-ordinate directions respectively
$\Theta_x, \Theta_y, \Theta_z$	rotations about the axis, x,y and z respectively
F_x, F_y, F_z	forces in the x,y and z directions respectively
M_x, M_y, M_z	moments at a node of an element about the x,y and z axis respectively
σ_x, σ_y	direct stresses in the x and y directions respectively
σ_{xy}	shear stress in x and y plane
q	displacement vector of an element in local co-ordinates
F	force vector of an element in local co-ordinates
Q	displacement vector of the assembled structure in global co-ordinates
P	force vector of the assembled structure in global co-ordinates
$\left[K_E^e\right]$	elastic stiffness matrix of an element
$\left[K_G^e\right]$	geometric stiffness matrix of an element
$\left[K\ \right]$	stiffness of the assembled structure

superscripts p and b refer to the in-plane and bending components associated with in-plane K_E^{ep} and bending K_E^{eb} stiffness matrices. Other symbols are defined as they occur.

BIBLIOGRAPHY

1. Timoshenko, S.P., and Gere, J.M., "Theory of Elastic Stability", McGraw-Hill, Tokyo.
2. Bleich, F., "Buckling Strength of Metal Structures", McGraw-Hill, New York (1952).
3. Girkmann, K., "Stability of the Webs of Plate Girders Taking Account of Concentrated Loads", Final Report, International Association for Bridge and Structural Engineering, 1936.
4. Zetlin, L., "Elastic Instability of Flat Plates Subjected to Partial Edge Loads", Proceedings, ASCE, vol. 81, September, 1955.
5. White, R.N., and Cottingham, W., "Stability of Plates Under Partial Edge Loading", Journal of the Engineering Mechanics Division, ASCE, vol. 88, No. EM5, Proc. Paper 3297, Oct., 1962, pp. 67-86.
6. Bossert, T.W., and Ostapenko, A., "Buckling and Ultimate Loads for Plate Girder Web Plates Under Edge Loading", Report No. 319.1, Fritz Engineering Laboratory, June, 1967.
7. Rockey, K.C., and Bagchi, D.K., "Buckling of Plate Girder Webs Under Partial Edge Loadings", International Journal of Mechanical Sciences, Pergamon Press, London, England, vol. 12, 1970, pp. 61-76.
8. Khan, M.Z., and Walker, A.C., "Buckling of Plates Subjected to Localized Edge Loading", The Structural Engineer, vol. 50, p.225-232.
9. Rockey, K.C., El-gaaly, M.A., and Bagchi, D.K., "Failure of Thin Walled Members Under Patch Loading", Journal of the Structural Division, ASCE vol. 98, No. ST12, Proc. Paper 9409, December, 1972, pp. 2739-2752.
10. Skaloud, M., "UNOSMOST A. Mechanismus ZHROUCENI., Temkych STEN Namahanych Osameym Bremenem", p. 452-465. Stavebmicky CASOPSIS SAV XX16-8, Bratislava, 1973.
11. Skaloud, M., and Novak, P. "Post Buckled Behaviour and Incremental Collapse of Webs Subjected to Concentrated Loads", I.A.B.S.E., 9th Congress, Amsterdam, 1972, p.101-110.
12. Bergfelt, A., "Studies and Tests on Slender Plate Girders Without Stiffeners, Shear Strength and Local Web Crippling", p.67-83, Proceedings, I.A.B.S.E. Colloquium "Design of Plate and Box Girders for Ultimate Strength", London, 1971.
13. Bergfelt, A., and Lindgren, S., "Livintryckning Under Koncentrerad Last Vid Balkar Med Slankt Liv", Chalmers Technical University, Report S74:5, 1975.

14. Timoshenko, S.P., "Theory of Plates and Shells", McGraw-Hill Ltd, New York.

15. Bagchi, D., "Large Deflection and Stability of Structural Members", Ph.D. Thesis, University of Wales (1969).

16. Zienkiewicz, O.C., and Cheung, Y.K., "The Finite Element Method in Structural and Continuum Mechanics", McGraw-Hill Ltd., London, 1967.

17. Yamaki, N., "Post-buckling Behaviour of Rectangular Plates with Small Initial Curvature Loaded in Edge Compression", J.App.Mech., vol. 26, pp. 407-414 (1959).

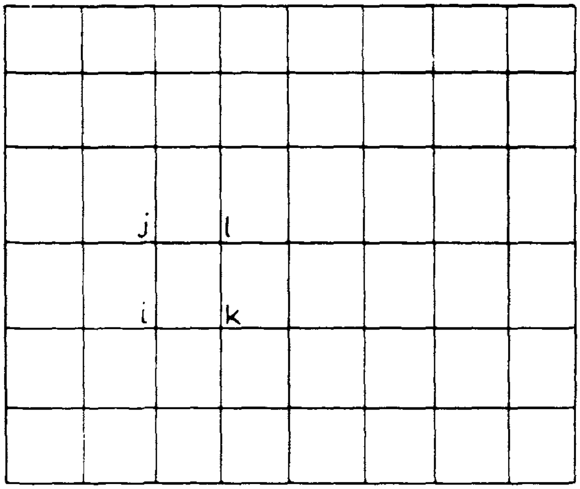

FIG. 1a. IDEALIZATION INTO FINITE ELEMENTS

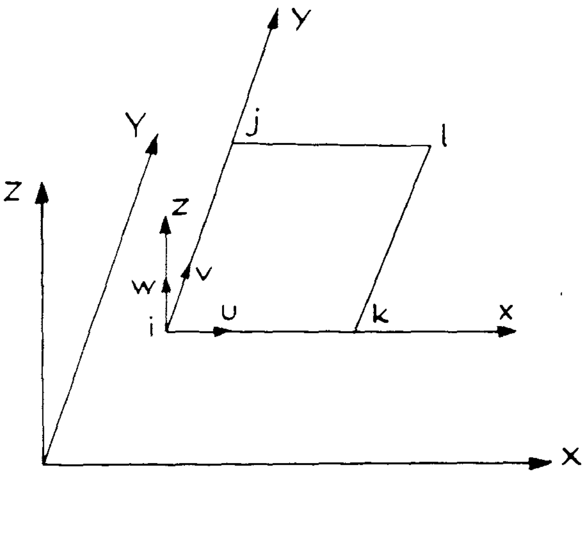

FIG. 1b. DESCRIPTION OF CO-ORDINATE SYSTEM

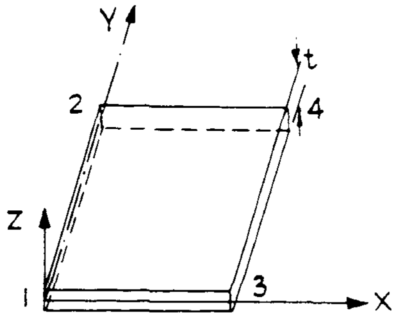

Sequence of node numbers

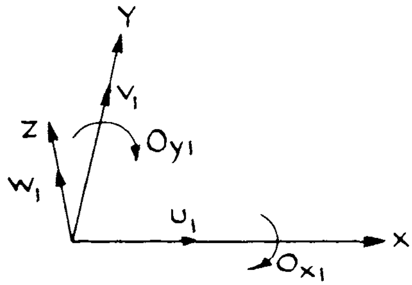

Degrees of freedom at a node

FIG. 2 SEQUENCE OF NODE NUMBERS & DEGREES OF FREEDOM AT A NODE

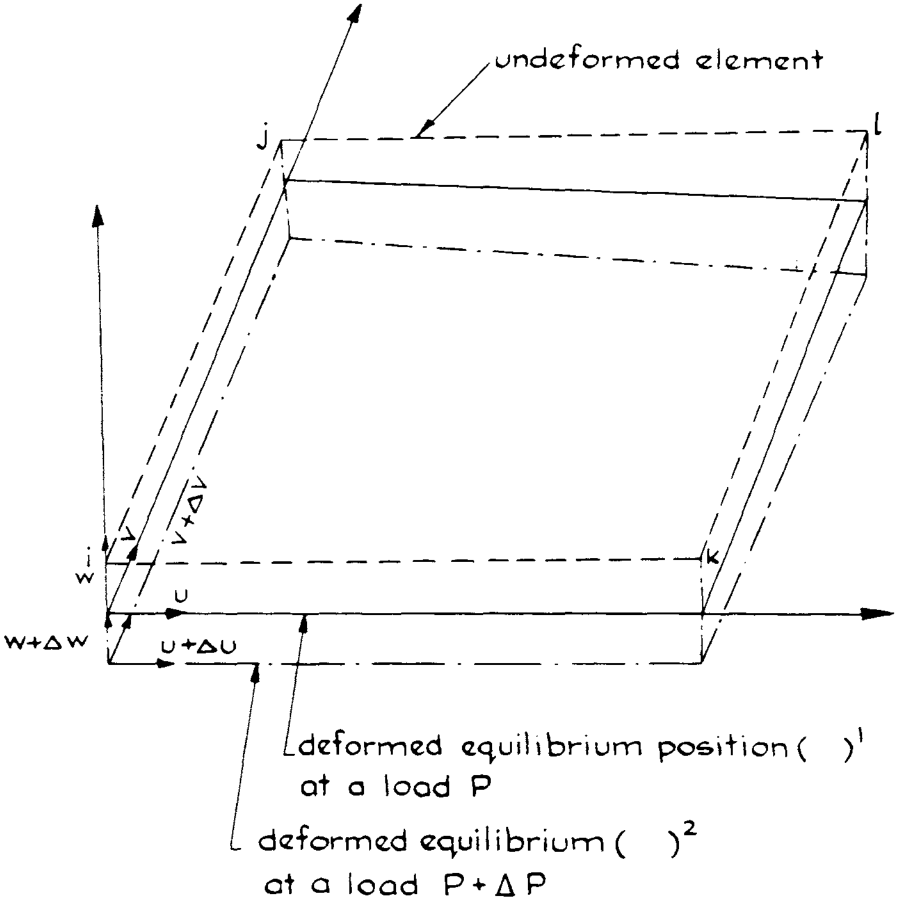

FIG. 3 VIEW OF A TYPICAL DEFORMED MODEL

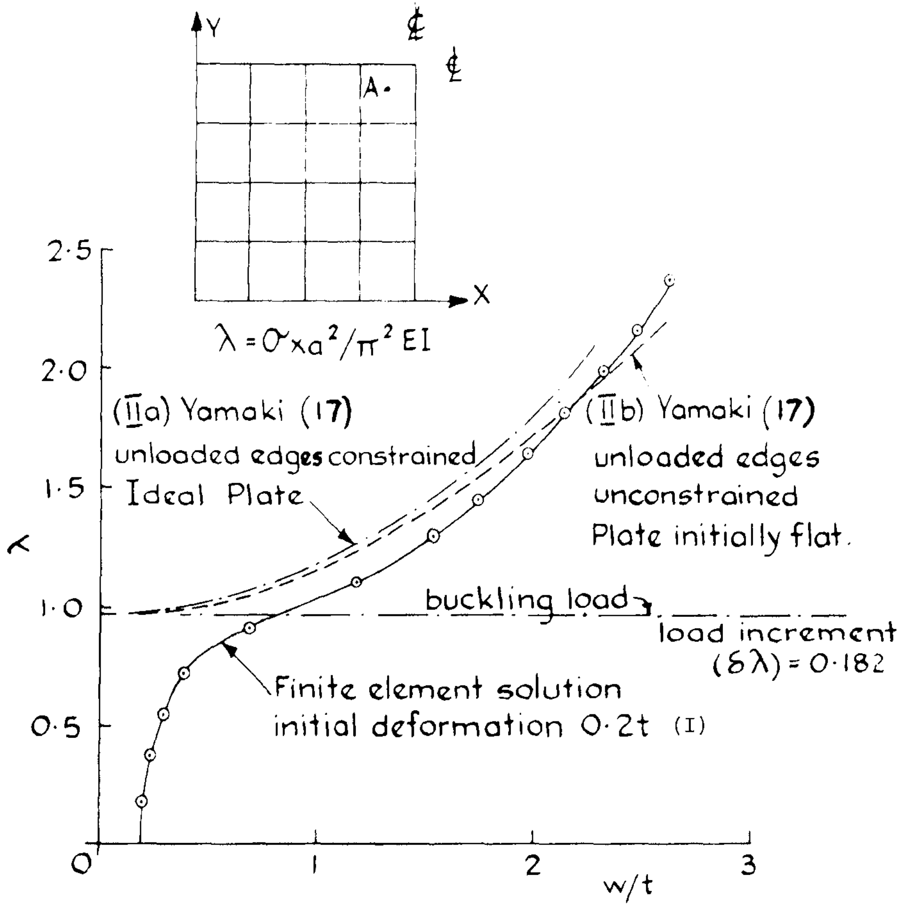

FIG. 4 POST-BUCKLING BEHAVIOUR OF CLAMPED SQUARE PLATE.

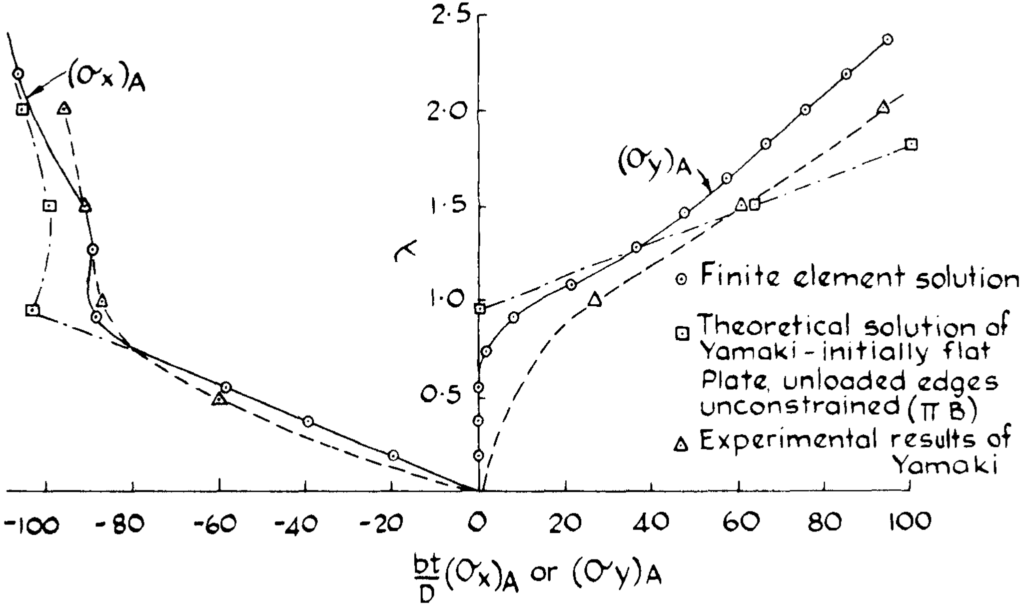

FIG. 5 CLAMPED SQUARE PLATE UNDER UNIFORM EDGE COMPRESSION MEMBRANE STRESS

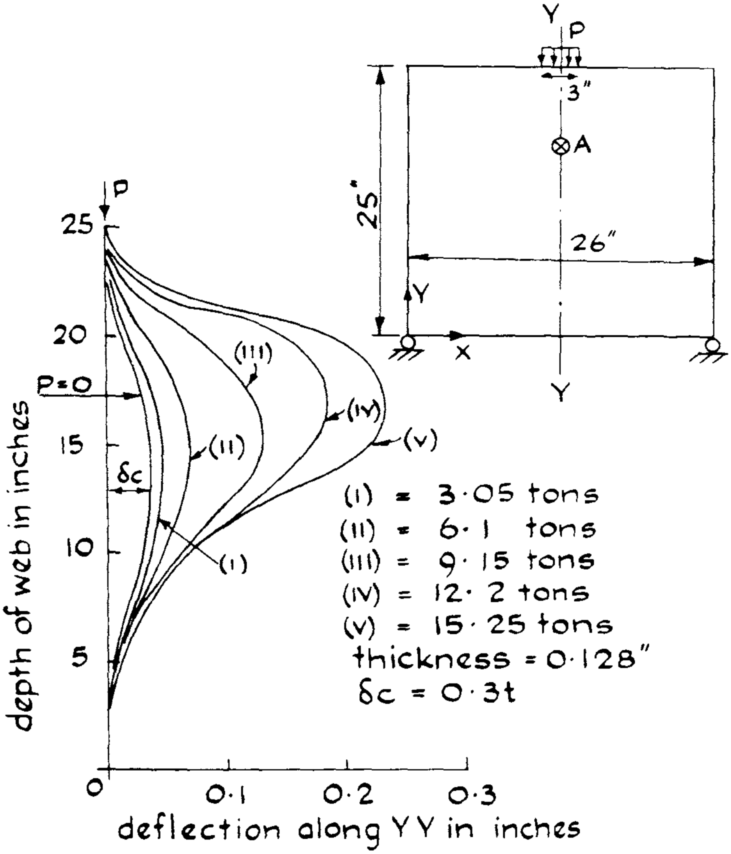

FIG. 6 POST-BUCKLING BEHAVIOUR OF A CLAMPED PANEL UNDER PARTIAL EDGE LOADING.

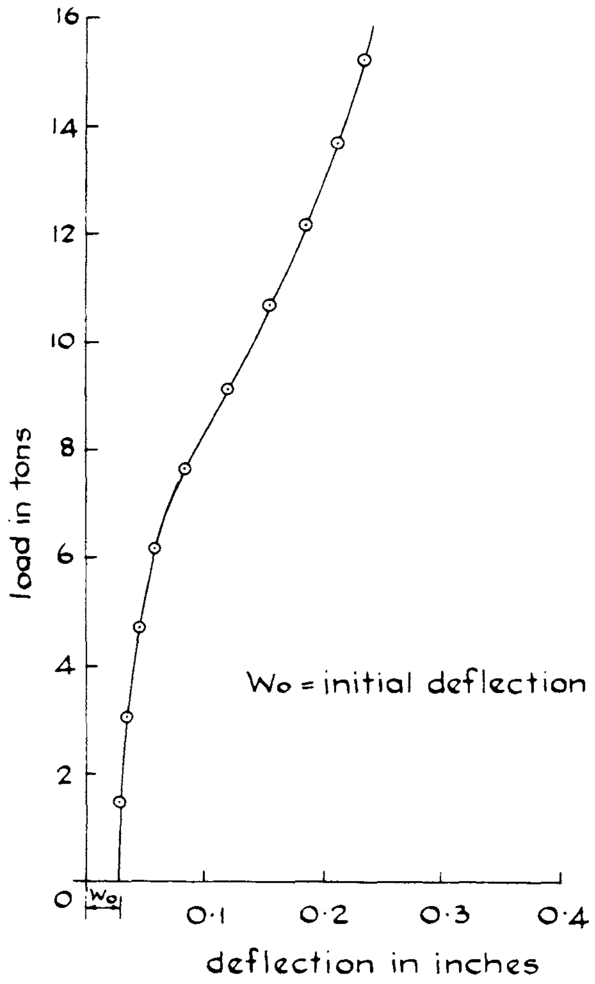

FIG. 7 LOAD/DEFLECTION BEHAVIOUR AT THE POINT MARKED A

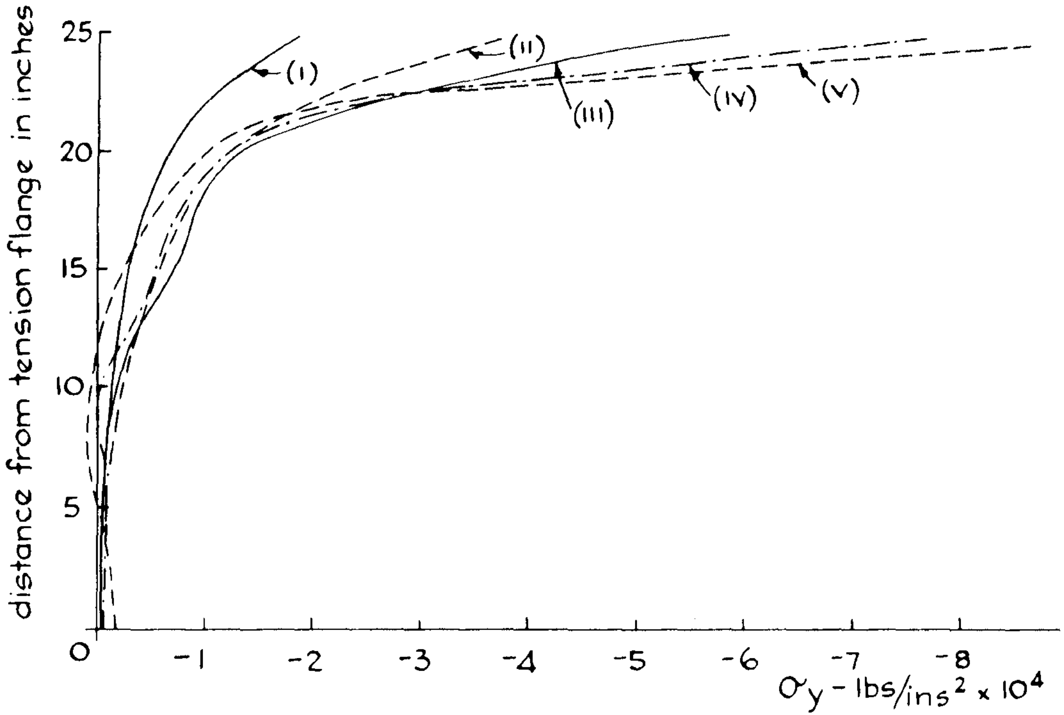

FIG. 8 MEMBRANE STRESS AT A DISTANCE OF 0·625 INCH FROM THE CENTRAL VERTICAL LINE

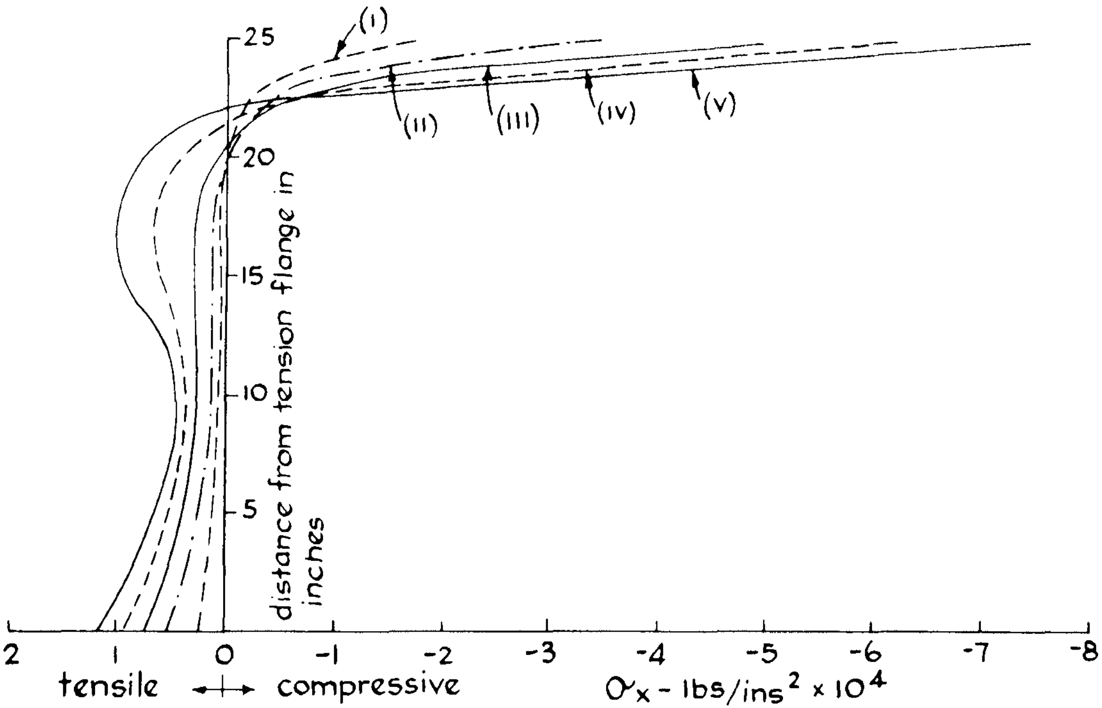

FIG. 9 MEMBRANE STRESS AT A DISTANCE OF 0·625 INCH FROM THE CENTRAL VERTICAL LINE.

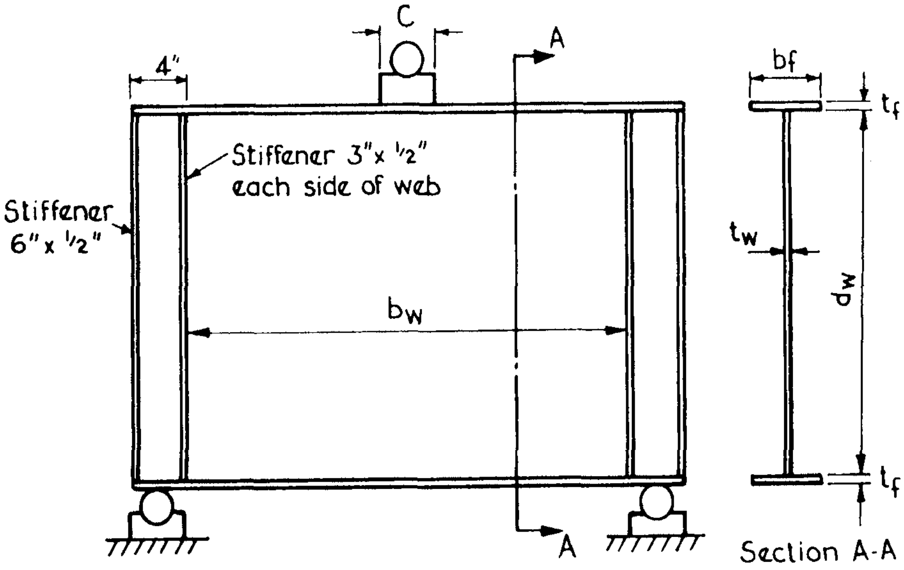

Girder Nº	dw in.	tw in.	bw in	bf in.	tf in.	C in.
B1.	25	0·128	34	6	0·5	2
B2	25	0·128	50	6	0·5	2
B3	25	0·128	26	6	0·5	3

Fig.10. Details of Test Girders.

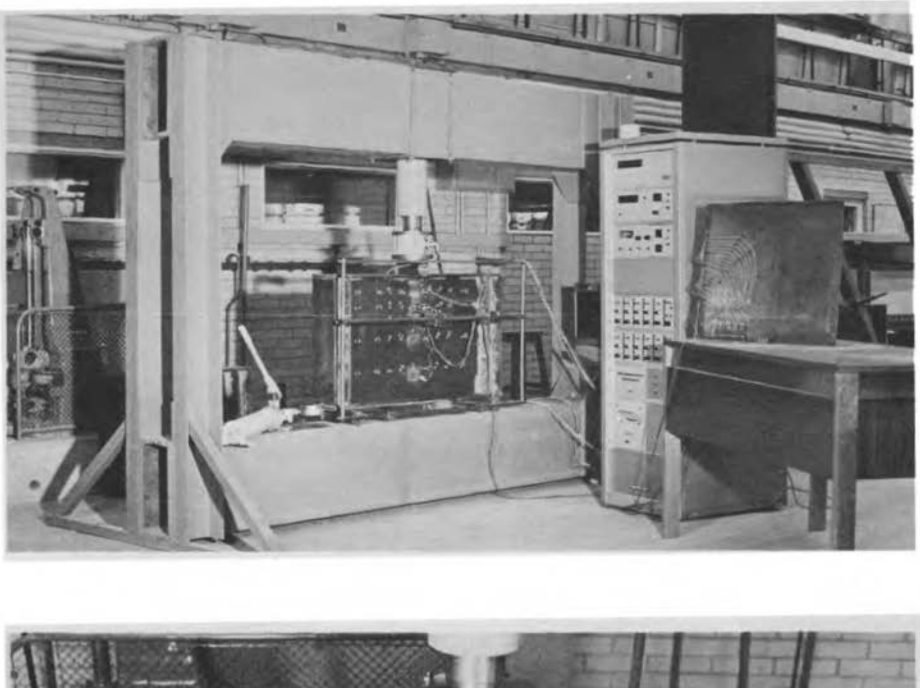

(b)

Figure 11. VIEW OF GIRDER IN TEST FRAME

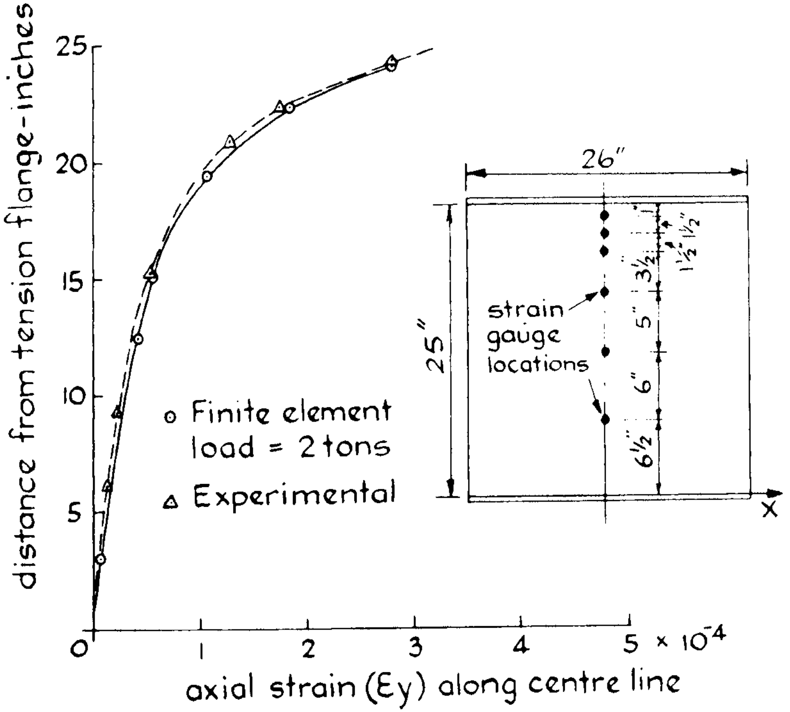

FIG. 12 COMPARISON OF EXPERIMENTAL VALUES OF MEMBRANE STRAIN ($\mathcal{E}y$) WITH FINITE ELEMENT SOLUTION

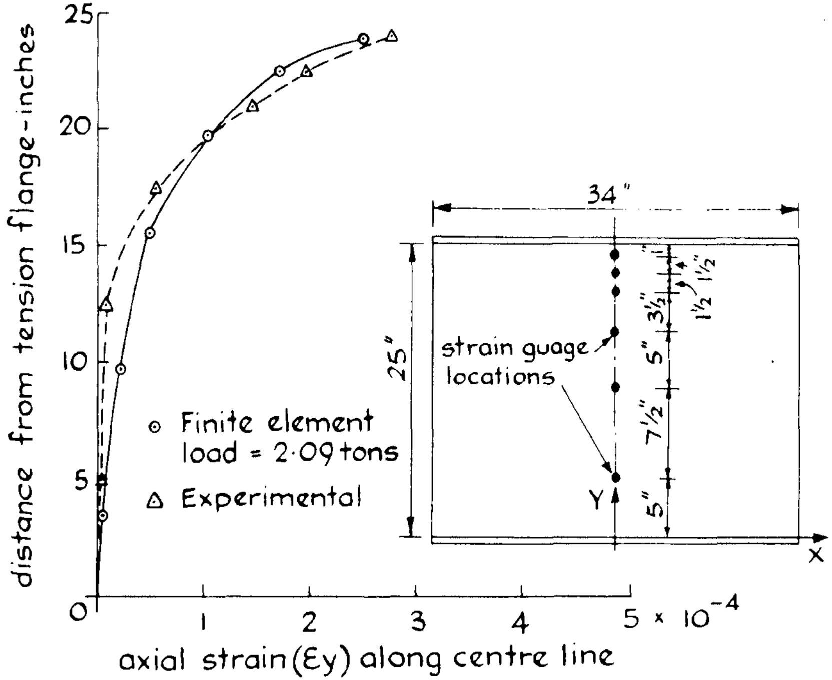

FIG. 13 COMPARISON OF EXPERIMENTAL VALUES OF MEMBRANE STRAIN (ε_y) WITH FINITE ELEMENT SOLUTION

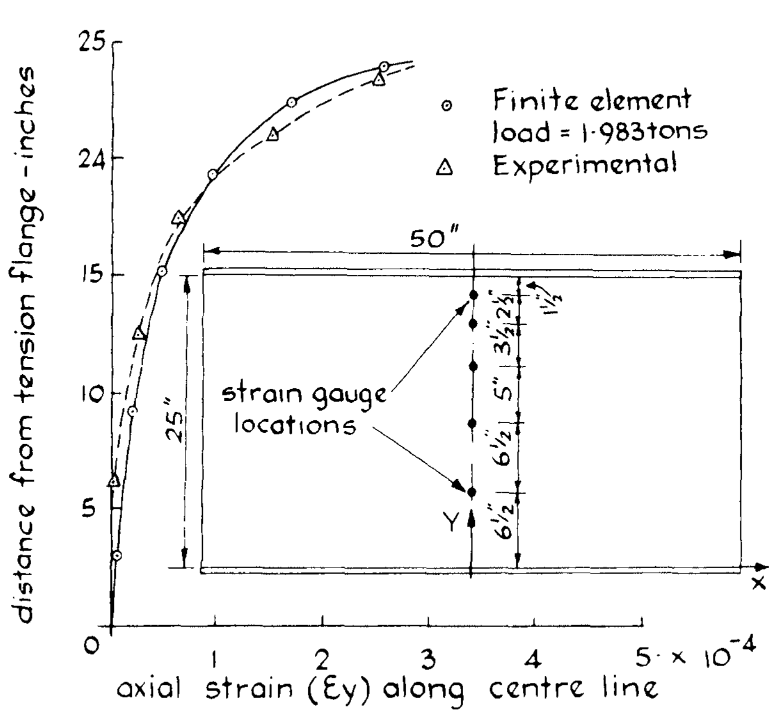

FIG 14 COMPARISON OF EXPERIMENTAL VALUES OF MEMBRANE STRAIN (ε_y) WITH FINITE ELEMENT SOLUTION

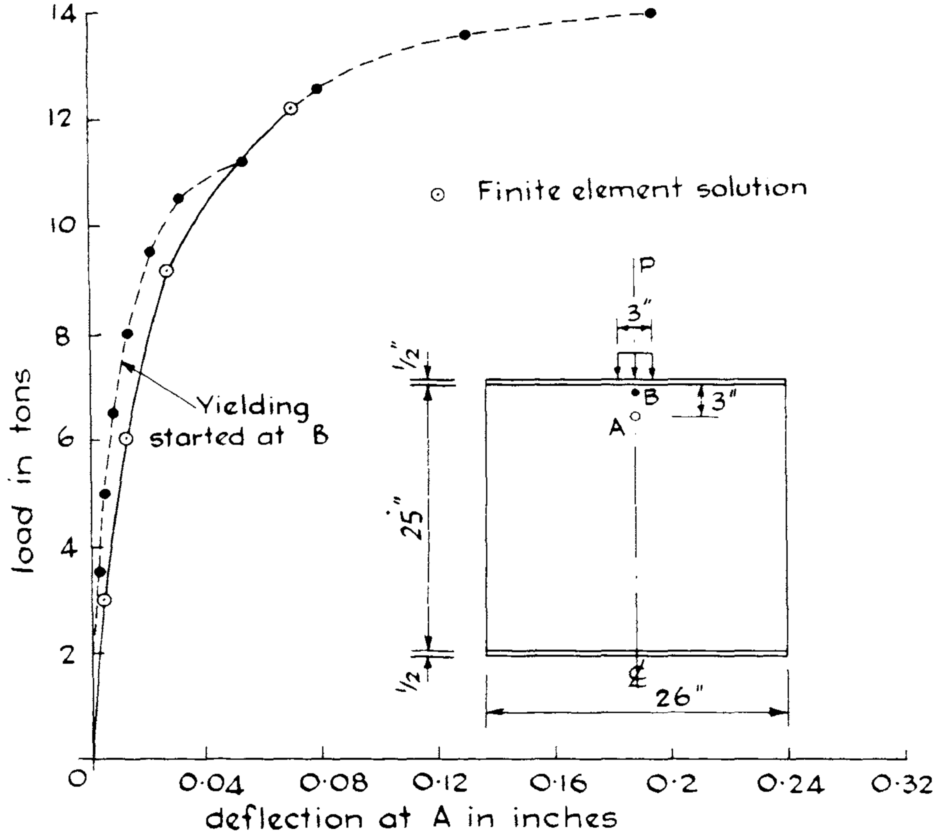

FIG. 15 LOAD/DEFLECTION BEHAVIOUR AT THE POINT MARKED A

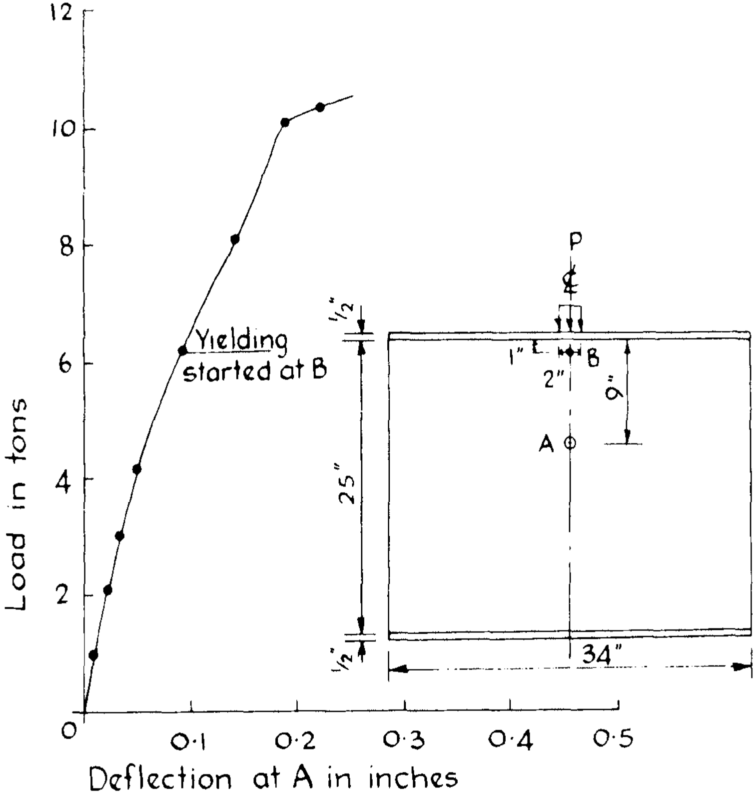

FIG. 16 LOAD/DEFLECTION BEHAVIOUR AT THE POINT MARKED A

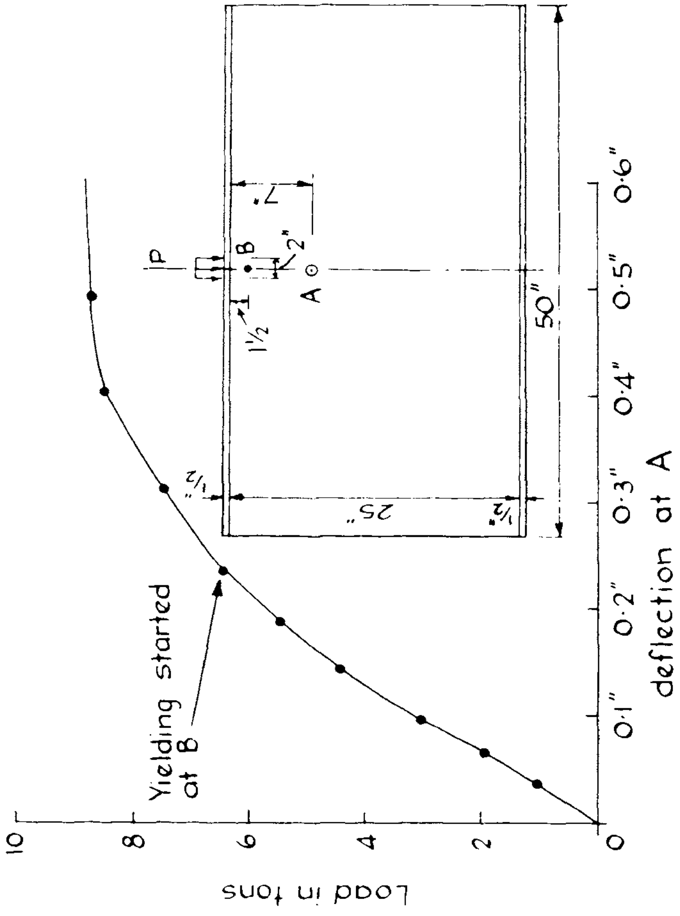

FIG. 17 LOAD DEFLECTION BEHAVIOUR AT THE POINT MARKED A